

X-Ray Diffraction Studies on the Structures of Tetraammine- and Triamminemonochlorozinc(II) Ions in Aqueous Solution

Toshio YAMAGUCHI and Hitoshi OHTAKI*

*Department of Electronic Chemistry, Tokyo Institute of Technology at Nagatsuta,
Nagatsuta-cho, Midori-ku, Yokohama 227*

(Received April 14, 1978)

X-Ray scattering measurements have been carried out on ammoniacal aqueous solutions of zinc(II) chloride at the NH_3/Zn mole ratios of 3.8, 5.0, and 6.6. The radial distribution curves show that the tetraamminezinc(II) complex is formed as the main species, the ammonia molecules within the complex being tetrahedrally coordinated to zinc(II) ion at a distance of (2.03 ± 0.02) Å. Analysis of the radial distribution curve obtained for the solution at the NH_3/Zn ratio of 3.8 indicates formation of the mixed complex $\text{ZnCl}(\text{NH}_3)_3^+$, the $\text{Zn}-\text{NH}_3$ and $\text{Zn}-\text{Cl}$ bond lengths being (2.00 ± 0.03) and (2.30 ± 0.03) Å, respectively.

According to the results of formation constants,¹⁾ enthalpic and entropic measurements¹⁾ and spectrophotometry,²⁾ a zinc(II) ion combines with four ammonia molecules at most, the structure of the tetraamminezinc(II) complex presumably being in a tetrahedral form. However, no X-ray crystallographic data are available because of the difficulty in the preparation of a stable single crystal.

In the present investigation we have attempted to determine the structure of the tetraamminezinc(II) complex as well as other zinc(II)-ammine complexes in ammoniacal aqueous solutions with various NH_3/Zn mole ratios (3.8, 5.0, and 6.6) by the X-ray diffraction method. Raman spectroscopic measurements were also carried out as a supplement to the structural determination of the main complex.

Experimental

Preparation and Analysis of Sample Solutions. The sample solutions were prepared by dissolving zinc(II) chloride (Wako Pure Chemicals, Co., reagent grade), which had been recrystallized twice from water, in a concentrated aqueous ammonia solution (Wako Pure Chemicals, Co., reagent grade, 28%). The concentration of ammonia was adjusted to the desired value by introducing gaseous ammonia (99.99%) into the sample solutions.

The concentration of zinc(II) ion was determined by EDTA titration and electrogravimetry. The results obtained by the two methods were found to agree with each other within 0.2%. Ammonia content in the sample solutions was determined by the Kjeldahl method. Concentration of the chloride ion was determined from the stoichiometry of the zinc(II) chloride.

The density of the solutions was determined pycnometrically.

The composition of the sample solutions is given in Table 1.

X-Ray Scattering Measurements. X-Ray scattering measurements were carried out by using a θ - θ JEOL diffractometer in a room thermostated at (25 ± 1) °C. Mo $K\alpha$ Radiation ($\lambda = 0.7107$ Å) was used. The diffracted beam was monochromatized with a Johansson-type LiF crystal and then a pulse height analyzer. The accessible range of scattering angle (2θ) was 2–140°, corresponding to the range $0.31 \text{ Å}^{-1} < s < 16.6 \text{ Å}^{-1}$ ($s = 4\pi\lambda^{-1} \sin \theta$). The time required for counting 40000 counts was recorded at each angle. The measurements over the whole angle range were carried out twice for each solution. The divergence of the measured intensities was within $\pm 2\%$. The average intensities thus measured at each scattering point were used in

the subsequent calculations. Details of the measurements are described in previous papers.^{3,4)}

Raman Spectroscopic Measurements. Raman spectra for the sample solutions were measured with a JEOL laser Raman spectrophotometer JRS-S1 with use of the 4880 Å excited line of Ar^+ laser.

Treatment of Intensity Data. The measured intensities $I(s)$ were corrected in the usual way for absorption and polarization of the X-ray beam.^{3–5)} The corrected intensities were normalized to electron units by the conventional methods,^{6,7)} from which the incoherent scatterings $\sum n_i \phi(s) I_i^{\text{inco}}(s)$ were subtracted (n_i = the number of atom i , $\phi(s)$ = the fraction of the incoherent radiation reaching the counter). The Breit-Dirac effect was taken into account. Correction for double scattering⁸⁾ was made, which did not exceed 4% of scattered intensities of solutions investigated. The values of coherent, incoherent and anomalous scatterings of all atoms were the same as those used previously⁹⁾ except for N, the values of which were taken from the literature.¹⁰⁾ The coherent intensities $I^{\text{coh}}(s)$ thus obtained are shown in Fig. 1 for each sample solution.

The radial distribution function $D(r)$ was calculated by

$$D(r) = 4\pi r^2 \rho_0 + \frac{2r}{\pi} \int_0^{s_{\text{max}}} s i(s) M(s) \sin(rs) ds, \quad (1)$$

where ρ_0 is the average scattering density in the stoichiometric volume V containing one Zn atom, s_{max} the maximum s -value attained in the measurements ($s_{\text{max}} = 16.7 \text{ Å}^{-1}$). $M(s)$ represents the modification function

$$\begin{aligned} & [\sum n_i \{ (f_i(0) + \Delta f_i')^2 + (\Delta f_i'')^2 \} / \sum n_i \{ (f_i(s) + \Delta f_i')^2 \\ & + (\Delta f_i'')^2 \}] \exp(-0.01s^2), \end{aligned} \quad (2)$$

where $f_i(0)$ and $f_i(s)$ denote the scattering factors of atom i at angle 0 and s , respectively. $\Delta f_i'$ represents the real part of the anomalous dispersion, whereas $\Delta f_i''$ is the imaginary one. The reduced intensity $i(s)$ is given by

$$i(s) = I^{\text{coh}}(s) - \sum n_i \{ (f_i(s) + \Delta f_i')^2 + (\Delta f_i'')^2 \}. \quad (3)$$

Before the Fourier transform, the reduced intensities experimentally obtained were smoothed by use of spline function.¹¹⁾ Spurious peaks appearing below 1 Å in the radial distribution curves were eliminated by the reported method.⁹⁾ Curve (a) in Fig. 2 represents the $(D(r) - 4\pi r^2 \rho_0)$ curve obtained by a Fourier transform of the reduced intensities of solution C after a correction for only spurious peaks within the hard-core radius (< 1 Å). The curve still shows periodic ripples in the range of large r values. The ripples were eliminated when the intensity data were further corrected by the smoothing procedure (Fig. 2, curve (b)). Thus, the data-smoothing procedure in combination with a hard-core correction is needed to correct spurious peaks in $D(r)$

TABLE 1. THE COMPOSITION (g-atoms/dm³) AND STOICHIOMETRIC VOLUME V PER ZINC ATOM IN THE SOLUTIONS

Solution	Zn	Cl	N	O	H	$\frac{\text{NH}_3}{\text{Zn}}$	$\frac{V}{\text{\AA}^3}$	Density g cm ⁻³
A	2.679	5.359	10.09	37.99	106.3	3.8	619.7	1.217
B	2.364	4.727	11.79	32.30	99.96	5.0	702.4	1.170
C	2.217	4.434	14.66	32.61	109.2	6.6	749.0	1.139

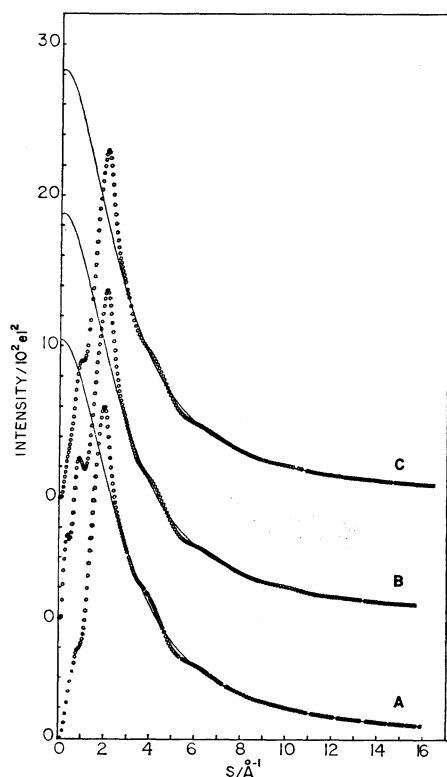


Fig. 1. X-Ray diffraction patterns for the sample solutions A, B, and C. Experimental coherent scattering intensities $I^{\text{coh}}(s)$ are shown by circles and calculated independent scattering intensities by solid lines.

curves over the whole angle range measured. It should be noted that the smoothing procedure leads sometimes to erroneous results when the intervals between data points are large. The separation between the points should be less than 0.3 \AA^{-1} in s . For solutions containing heavy atoms the smoothing correction for the scattered intensities might be unnecessary.

The $s \cdot i(s)$, $D(r)$, and $(D(r) - 4\pi r^2 \rho_0)$ curves obtained after the smoothing correction are shown in Figs. 3, 4, and 5, respectively, for each solution.

The theoretical peak shape of an atom pair i - j was estimated from the calculated reduced intensity:

$$i_{\text{calc}}(s) = n_{ij} \{ (f_i(s) + \Delta f_i') (f_j(s) + \Delta f_j') + (\Delta f_i'') (\Delta f_j'') \} \times \frac{\sin(r_{ij}s)}{(r_{ij}s)} \exp(-b_{ij}s^2), \quad (4)$$

where r_{ij} , b_{ij} , and n_{ij} denote the distance, the temperature factor and the frequency factor of the atom pair i - j , respectively.

All calculations were performed with the aid of electronic computers HITAC 8700 and M 180 by means of the KUR-VLR program.¹²⁾

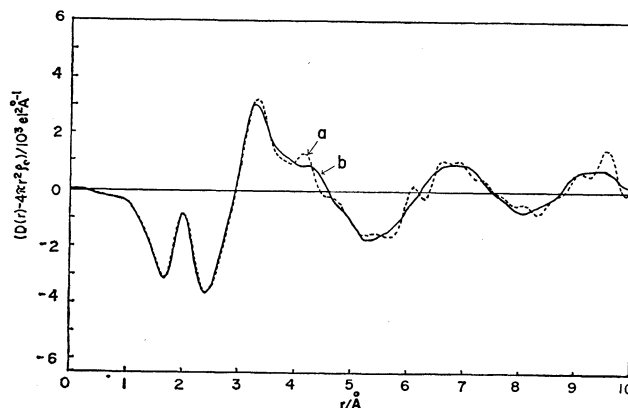


Fig. 2. The $(D(r) - 4\pi r^2 \rho_0)$ curves obtained after the hard-core correction alone (curve (a)) and further data-smoothing correction (curve (b)) for solution C.

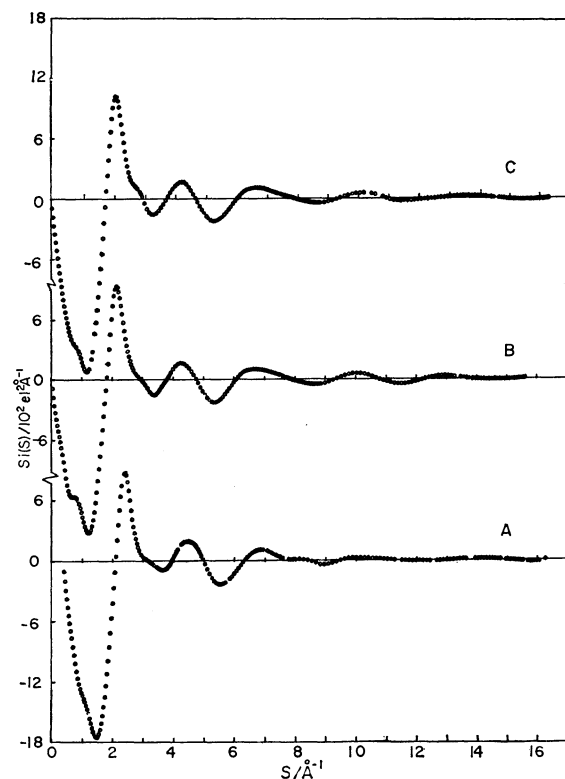


Fig. 3. The reduced intensities $i(s)$ multiplied by s for solutions A, B, and C.

Results and Discussion

Structure of Tetraamminezinc(II) Ion. Solutions B and C (Table 1) predominantly contain the tetraamminezinc(II) complex according to the formation con-

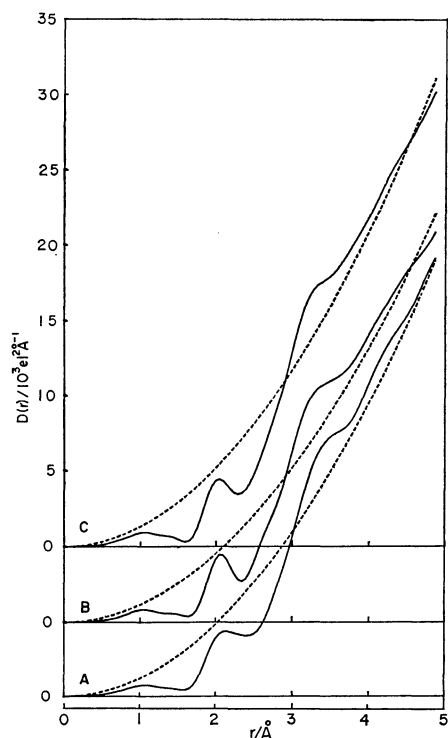


Fig. 4. The radial distribution curves, $D(r)$, for solutions A, B, and C. The curves of $4\pi r^2 \rho_0$ are shown by dashed lines.

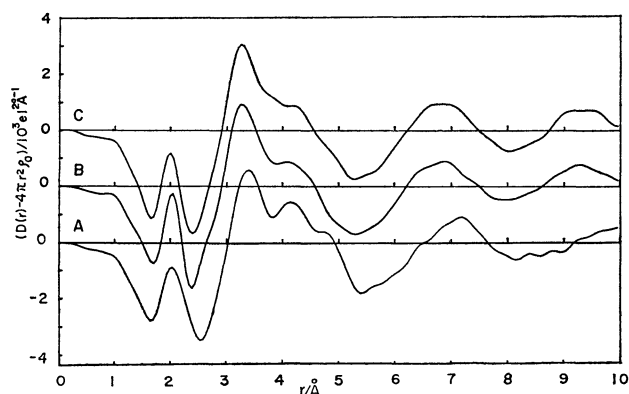


Fig. 5. The $(D(r) - 4\pi r^2 \rho_0)$ curves for solutions A, B, and C.

stants so far reported.¹⁾ Therefore, the data obtained from these solutions are assessed to the tetraamminezinc(II) species rather than triammineaquazinc(II) and other amminezinc(II) complexes, although nitrogen and oxygen atoms coordinated to the metal ion are undistinguishable by the X-ray method. In each $D(r)$ curve four peaks appear around 1.0, 2.0, 3.3, and 4.2 Å (Fig. 4). The small and broad peak at about 1.0 Å is due to the O-H bonds in water. The N-H bonds in ammonia molecules may partly contribute to the peak. The second peak located at 2.0 Å can be ascribed to the interaction between the zinc(II) ion and the nearest ammonia molecules as is expected from the sum of the sizes of a Zn^{2+} ion and an ammonia molecule. The third peak at about 3.3 Å is mainly due to the Cl-O contacts.¹³⁻¹⁶⁾ The fourth peak found

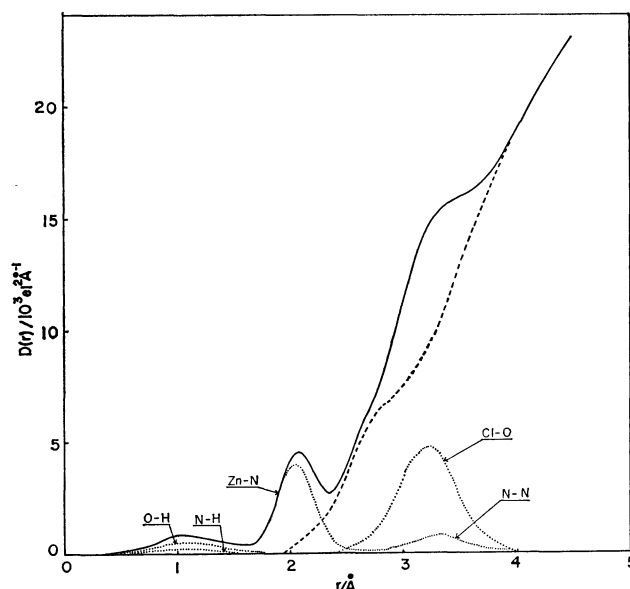


Fig. 6. The radial distribution curve for solution B. The dashed line shows the residual curve after subtraction of the theoretical peaks calculated for the O-H and N-H bonds within H_2O and NH_3 , the Zn-N and N...N contacts within $\text{Zn}(\text{NH}_3)_4^{2+}$ and the Cl-O pair within $\text{Cl}(\text{H}_2\text{O})_6^-$ from $D(r)$ curve.

around 4.2 Å may be due to the interactions between the zinc(II) ion and the molecules in the second coordination sphere.¹⁷⁾

The $D(r)$ curve of solution B is essentially the same as that of solution C. The area under the peak at 2.0 Å gives about four ammonia molecules bonded to the zinc(II) ion. The area and the location of the peak rule out the existence of the $\text{Zn}(\text{NH}_3)_4(\text{OH}_2)_2^{2+}$ species of the octahedral form and the formation of the contact ion pair between zinc(II) and chloride ions, the peak maximum due to the Zn-Cl atom pair being expected to appear at about 2.3 Å.¹⁶⁾ The position and the area of the peak are not affected by increase in the NH_3/Zn ratio. The Zn-N bond length within the tetraamminezinc(II) ion was determined by the trial-and-error method so as to obtain a smooth background curve with no indication of any other intramolecular interactions within the first coordination layer of the zinc(II) ion. The temperature factor calculated from the half-width of the peak at 2.0 Å in $D(r)$ was 0.002–0.003 Å², which is in good agreement with 0.0022 Å² obtained from spectroscopic data.¹⁸⁾ The length of the Zn-N bond was finally determined to be (2.03 ± 0.02) Å. The results are shown in Fig. 6, together with the contribution from the hydrated chloride ion to the $D(r)$ curve calculated by using the distance and the temperature factor of the Cl-O bond within the $\text{Cl}(\text{H}_2\text{O})_6^-$ ion reported by Narten *et al.*¹³⁾ There is no appreciable peak in the residual curve (Fig. 6, dashed line) in the range $r < 4$ Å except for a broad peak around 2.8 Å which corresponds to the adjacent O-O bond of bulk water and N-O bond of dissolved ammonia.¹⁹⁾

Structure of Triamminemonochlorozinc(II) Ion. Solution A might contain a small amount of triammine-

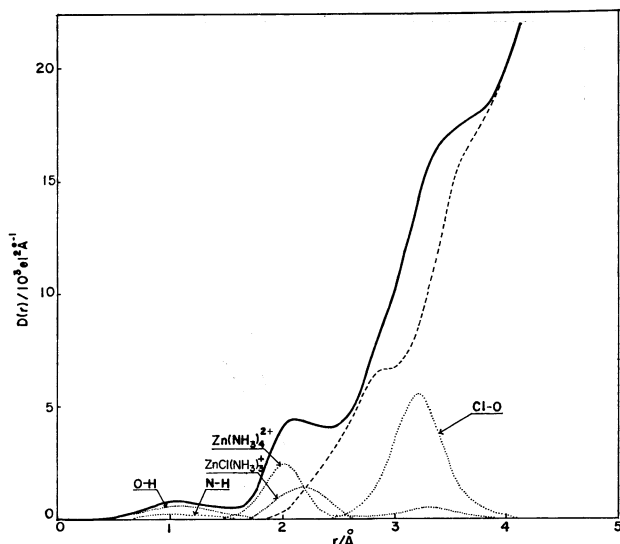
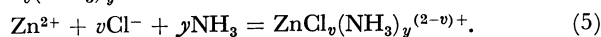


Fig. 7. The radial distribution curve for solution A. The dashed line shows the difference between the $D(r)$ curve and theoretical peak shapes calculated for the O-H and N-H bonds within H_2O and NH_3 , the Zn-N and N...N contacts within $\text{Zn}(\text{NH}_3)_4^{2+}$, the Zn-N and Zn-Cl bonds within $\text{ZnCl}(\text{NH}_3)_3^+$ and Cl-O pair within $\text{Cl}(\text{H}_2\text{O})_6^-$.

zinc(II) complex besides the predominant tetraamminezinc(II) ion. Since the solution contains a large amount of chloride ions, mixed chloro-ammine complexes may be formed in the solution. Although no formation constants of the mixed chloro-ammine complexes of zinc(II) ion have been reported, the formation constants can be estimated by an appropriate equation for the formation equilibria of the mixed complexes. The equilibrium for the formation of a mixed complex $\text{ZnCl}_v(\text{NH}_3)_y^{(2-v)+}$ is written as follows:



If we use Dyrssen's equation²⁰⁾ for the calculation of the equilibrium constant of the complex, we obtain β_{1vy} as follows:

$$\log \beta_{1vy} = \log \frac{(v+y)!}{v!y!} + \frac{v}{v+y} \log \beta_{1,v+y,0} + \frac{y}{v+y} \log \beta_{1,0,v+y}, \quad (6)$$

where the constant β_{1vy} is defined as $[\text{ZnCl}_v(\text{NH}_3)_y]^{(2-v)+} / [\text{Zn}^{2+}][\text{Cl}^-]^v[\text{NH}_3]^y$. Thus, the stepwise formation constant $K = [\text{ZnCl}(\text{NH}_3)_3^+] / [\text{Zn}(\text{NH}_3)_3^{2+}][\text{Cl}^-]$ is given by

$$\text{Zn}(\text{NH}_3)_3^{2+} + \text{Cl}^- = \text{ZnCl}(\text{NH}_3)_3^+, \quad K = \beta_{113} / \beta_{103}. \quad (7)$$

The value of β_{113} was estimated by insertion of the values of β_{104} and β_{140} ¹⁾ into Eq. 6 (β_{103} was also quoted from the same literature). The stepwise formation constant K thus evaluated was 1.2. The composition of solution A was estimated to be 60 mol % of $\text{Zn}(\text{NH}_3)_4^{2+}$, 34 mol % of $\text{ZnCl}(\text{NH}_3)_3^+$ and 6 mol % of $\text{Zn}(\text{NH}_3)_3(\text{OH}_2)^{2+}$.

The theoretical peaks of the radial distribution curve of solution A were calculated on the basis of the com-

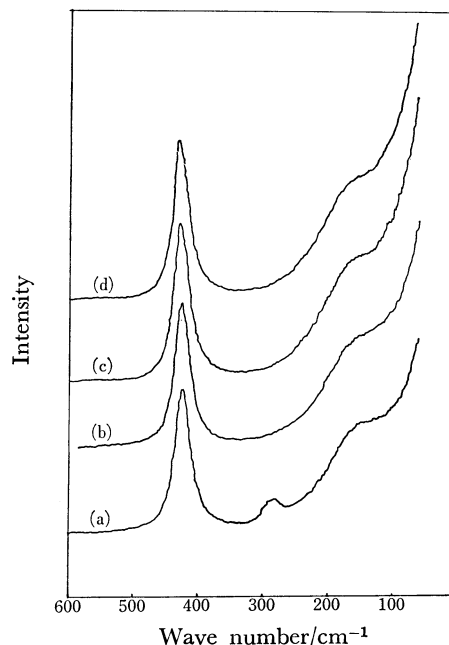


Fig. 8. Raman spectra of solutions. (a) Solution A; (b) solution B; (c) solution C; (d) solution at NH_3/Zn ratio=10.

position of the complexes. The peak shapes for each atom pair are shown in Fig. 7. The parameter values of the $\text{Zn}(\text{NH}_3)_4^{2+}$ ion used were those obtained in the previous section. The parameter values of the structure of the $\text{ZnCl}(\text{NH}_3)_3^+$ complex were obtained by the trial-and-error method. The formation of the $\text{Zn}(\text{NH}_3)_3(\text{OH}_2)^{2+}$ ion was neglected, because of its small amount and the structure practically undistinguishable from $\text{Zn}(\text{NH}_3)_4^{2+}$ by means of X-ray. The distances of the Zn-NH₃ and Zn-Cl bonds within the $\text{ZnCl}(\text{NH}_3)_3^+$ complex thus determined were (2.00 ± 0.03) and (2.30 ± 0.03) Å, respectively. The smooth background curve, except for a broad peak around 2.8 Å due to the structure of bulk water, indicates no significant intramolecular interaction being left within the first coordination shell of the zinc(II) ion.

Raman spectra have been observed in a solution containing the tetraamminezinc(II) ion²¹⁾ and in the solid $[\text{Zn}(\text{NH}_3)_4]\text{I}_2$ compound having the tetrahedral $\text{Zn}(\text{NH}_3)_4^{2+}$ moiety.²⁾ In aqueous solution the only totally symmetric Zn-NH₃ frequency was found at 428 cm⁻¹, the band being almost identical to the 431.2 cm⁻¹ band of the solid state. In the spectra of all the solutions A, B, and C, a totally symmetric Zn-NH₃ stretching vibration appeared at (429 ± 1) cm⁻¹ (Fig. 8). No change in the Raman spectrum was observed even in a solution of $\text{NH}_3/\text{Zn}=10$ prepared by introduction of gaseous ammonia into solution C. The results suggest that the tetraamminezinc(II) ion is the main species in solutions of an NH_3/Zn ratio larger than 3.8 and that no higher-ammine-zinc(II) complexes can be formed even in solutions of high ammonia content. In solution A, a small polarized band was observed at ca. 285 cm⁻¹ (Fig. 8). In Raman spectroscopic studies of zinc(II) chloride solution in the presence of ammonium chloride at various pH

values, Beer *et al.* assigned the band at 284 cm^{-1} observed for the solutions at high pH values to the Zn-Cl stretching frequency of the chloro-ammine complexes.²²⁾ Perchard and Novak²³⁾ reported on the Raman spectra of the $\text{ZnCl}_2(\text{NH}_3)_2$ crystal and assigned the bands at 420 and 283 cm^{-1} to the Zn-NH₃ and Zn-Cl stretching frequencies, respectively. The band around 285 cm^{-1} might be due to the symmetric Zn-Cl stretching vibration of the triamminemonochlorozinc(II) ion present in the solution, the Zn-N stretching frequency overlapping the 429 cm^{-1} band of the predominant tetraamminezinc(II) ion.

As is seen in Fig. 1, a small peak appears at about 0.8 \AA^{-1} in s in all the X-ray diffraction patterns. According to Dorosh and Skryshevskii²⁴⁾ and Marques and Marques,²⁵⁾ the peak is due to the "super-arrangement" of cations in the solution. The distance between the cations, R_c , is calculated by

$$R_c = 7.73/s_m, \quad (8)$$

where s_m denotes the s -value of the peak maximum. The distance R_c thus calculated is about 9 \AA , in good agreement with the calculated zinc(II)-zinc(II) distance from the stoichiometric volume given in Table 1. The distances are 8.5 , 8.9 , and 9.1 \AA for the solutions A, B, and C, respectively.

The present work was partially supported by a Grant-in-Aid for Scientific Research from the Ministry of Education.

References

- 1) L. G. Sillén and A. E. Martell, "Stability Constants," Spec. Publ. No. 17 and Supplement No. 1, Spec. Publ. No. 25, The Chemical Soc., London (1964) and (1971).
- 2) K. H. Schmidt and A. Müller, *Coord. Chem. Rev.*, **19**, 41 (1976).
- 3) H. Ohtaki and M. Maeda, *Bull. Chem. Soc. Jpn.*, **47**, 2197 (1974).
- 4) H. Ohtaki, M. Maeda, and S. Ito, *Bull. Chem. Soc. Jpn.*, **47**, 2217 (1974).
- 5) H. A. Levy, M. D. Danford, and A. H. Narten, ORNL-3960 (1966).
- 6) K. Furukawa, *Rep. Progr. Phys.*, **25**, 395 (1962).
- 7) J. Krogh-Moe, *Acta Crystallogr.*, **2**, 951 (1956).
- 8) B. E. Warren and R. L. Mozzi, *Acta Crystallogr.*, **21**, 459 (1966).
- 9) H. Ohtaki, T. Yamaguchi, and M. Maeda, *Bull. Chem. Soc. Jpn.*, **49**, 701 (1976).
- 10) D. T. Cromer and J. T. Waber, *Acta Crystallogr.*, **18**, 104 (1965); D. T. Cromer, *J. Chem. Phys.*, **50**, 4857 (1969); D. T. Cromer and D. Lieberman, *J. Chem. Phys.*, **53**, 1891 (1970).
- 11) K. Ichida, F. Yoshimoto, and T. Kiyono, *Joho Shori*, **15**, 414, 477 (1974).
- 12) G. Johansson and M. Sandström, *Chem. Scripta*, **4**, 195 (1973).
- 13) A. H. Narten, F. Vaslow, and H. A. Levy, *J. Chem. Phys.*, **58**, 5017 (1973).
- 14) D. L. Wertz, *J. Solution Chem.*, **1**, 489 (1972).
- 15) R. Caminiti, G. Licheri, G. Piccaluga, and G. Pinna, *J. Chem. Phys.*, **65**, 3134 (1976).
- 16) D. L. Wertz and J. R. Bell, *J. Inorg. Nucl. Chem.*, **35**, 37 (1973).
- 17) W. Bol, G. J. A. Gerrits, and C. L. van Panthaleon van Eck, *J. Appl. Crystallogr.*, **3**, 486 (1970).
- 18) S. J. Cyvin, B. N. Cyvin, and R. Andreassen, *J. Mol. Struct.*, **25**, 141 (1975).
- 19) A. H. Narten, *J. Chem. Phys.*, **49**, 1962 (1968).
- 20) D. Dyrssen, D. Janger, and F. Wengelin, "Computer Calculation of Ionic Equilibria and Titration Procedures," Almquist and Wiksell, Stockholm (1968).
- 21) K. Nakamoto, J. Takemoto, and T. L. Chow, *Appl. Spectrosc.*, **25**, 352 (1971).
- 22) J. Beer, D. R. Crow, R. Grzeskowiaki, and I. D. M. Turner, *Inorg. Nucl. Chem. Lett.*, **9**, 35 (1973).
- 23) C. Perchard and A. Novak, *Spectrochim. Acta, Part A*, **26**, 871 (1970).
- 24) A. K. Dorosh and A. F. Skryshevskii, *Russ. J. Struct. Chem.*, **8**, 300 (1966).
- 25) M. A. Marques and M. I. D. B. Marques, *Proc. N. Ned. Akad. Wet., Part B*, **77**, 286 (1974).